PHYSICAL REVIEW B VOLUME 27, NUMBER 8 15 APRIL 1983

Thermoreflectance test of W, Mo, and paramagnetic Cr band structures

E. Colavita
Istituto di Fisica "G. Marconi," Università degli Studi di Roma, I-00185 Roma, Italy
and Dipartimento di Fisica, Università degli Studi della Calabria, Arcavacata di Rende, I-87100 Cosenza, Italy
and Gruppo Nazionale di Struttura della Materia del Consiglio Nazionale delle Ricerche, Roma, Italy

A. Franciosi
Synchroton Radiation Center, University of Wisconsin—Madison, Stoughton, Wisconsin 53589

C. Mariani
Istituto di Fisica "G. Marconi," Università degli Studi di Roma, I-00185 Roma, Italy

R. Rosei
Istituto di Fisica "G. Marconi," Università degli Studi della Roma, I-00185 Roma, Italy
and Dipartimento di Fisica, Università degli Studi della Calabria, Arcavacata di Rende, I-87100 Cosenza, Italy
and Gruppo Nazionale di Struttura della Materia del Consiglio Nazionale delle Ricerche, Roma, Italy
(Received 4 November 1982)

We present a systematic investigation of the electronic structure of W, Mo, and paramagnetic Cr. Thermoreflectance has been used to test the most recent band-structure calculations. Analysis of the systematic trends and improvement of the experimental method allowed us to identify a number of new critical-point and Fermi-surface transitions. An unambiguous interpretation is given for most optical-absorption features in the $0.5 < h\nu < 5.0$ eV photon-energy range.

I. INTRODUCTION

The interpretation of the optical spectra of transition metals is a rather formidable task[1-3] since the experimental features are generally broad and the calculated band structures show a number of levels closely spaced in energy. Considerable effort has been devoted to study the static optical conductivity of these metals which leads to a better understanding of their electronic structure.[4] Intrinsic limitations of this technique, however, often prevent unambiguous identifications.

We performed a thermoreflectance investigation of bulk W,[5] Mo,[5] and Cr.[6] Results for antiferromagnetic and paramagnetic Cr are reported in detail elsewhere,[7] but the conclusions are used here extensively for the interpretation of the systematics. This work is a continuation of our effort to understand the electronic properties of transition metals.[1,7-9] In earlier studies we analyzed with the same technique the properties of group-VB metals[1] and of Nb_xMo_{1-x} alloys.[9] Our approach is threefold:

(1) Modulation techniques[10] were used together with static optical data to yield information on optical transitions in specific regions of K space. Thermoreflectance[7-9] emphasizes optical absorption at critical points in the Brillouin zone (BZ) and optical transitions involving the Fermi level.

(2) Bulk samples were used since strain in evaporated films gives rise to broadening of the experimental features. Thermoreflectance measurements generally show more detail for bulk samples[1] than for film spectra.[11]

(3) The systematic trends in the electronic structure of the transition metals were exploited in the interpretation of the optical properties.[12] Transition metals in the same row of the Periodic Table exhibit similar band structures, while the width of the d bands increase progressing downward along each column. Therefore, the *gross* variations of the spectral features are predictable *"a priori."*

Weaver *et al.*[13] and Dallaporta *et al.*[14] previously reported thermoreflectance data for Mo (Refs. 13 and 14) and W.[14] The authors[14] did not perform a Kramers-Kronig (KK) analysis of their data so that their tentative interpretation is only qualitative. Among the original results of the present study we mention the unambiguous identification of critical-point transitions at N and Fermi-surface transitions

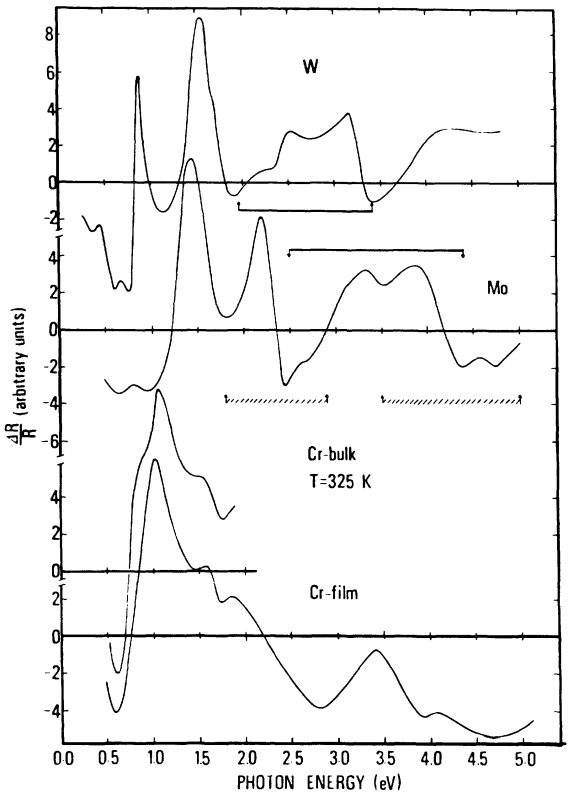

FIG. 1. Thermoreflectance spectra of W, Mo, and Cr. The $\Delta R/R$ spectra of Cr are taken from Refs. 7 and 11. The dashed intervals emphasize similar absorption features within the same Mo spectrum and for W as compared to Mo.

along Δ and Σ as dominant contributions to the optical absorption.

II. EXPERIMENTAL

The samples were single crystals (typically $2\times3\times0.2$ mm^3 in size) cut with a low-speed diamond saw and polished with abrasive. Mechanical damage was removed by heavy electropolishing with 6% perchloric acid in methanol at dry-ice temperature.

The temperature-induced relative change in the reflectivity $\Delta R/R$ was measured around an average sample temperature $\bar{T}=140$ K (for Mo and W) and at $\bar{T}=325$ K for paramagnetic Cr. The typical estimated temperature modulation ΔT around $\bar{T}$ was of 1–4 K. The experimental setup (including the optical and the electronic layout) has been described in detail elsewhere.[15]

Digital integration of the lock-in amplifier output was used to reduce the statistical uncertainty of $\Delta R/R$. Integration times up to 20–30 sec were necessary to reduce the indetermination below 3% over the whole energy range.

III. RESULTS

A. General overview

The measured $\Delta R/R$ spectrum for Cr, Mo, and W are shown in Fig. 1. The $\Delta R/R$ spectrum of Cr film from Ref. 11 is also shown for comparison. The temperature modulation ΔT scales all spectra and varies for each sample mounting, so that $\Delta R/R$ is given in arbitrary units. This is not important, however, since we consider only the spectral line shapes.

The results of Fig. 1 exhibit more fine structures than previously observed for film samples. The W and Mo spectra show clear similarities (see the energy intervals marked by arrows in Fig. 1) that may be indicative of similar absorption. Although a systematic trend is present in Fig. 1, the interpretation of $\Delta R/R$ alone is often misleading. $\Delta R/R$, in fact, is a complicated function of the complex dielectric function $\tilde{\epsilon}$. The most efficient way to interpret modulated optical spectra is correlating the temperature modulation of the dielectric function $\Delta\tilde{\epsilon}=\Delta\epsilon_1+\Delta\epsilon_2$ to specific interband transitions. Therefore, the $\Delta R/R$ spectra have been Kramers-Kronig analyzed to obtain the temperature variation of the real and imaginary part of the dielectric function ($\Delta\epsilon_1$ and $\Delta\epsilon_2$, respectively). Static dielectric functions from Refs. 2 and 16 were used in the KK analysis. The $\Delta R/R$ spectra were exponentially extrapolated to zero in the infrared and ultraviolet region in order to minimize the error induced by the finite width of the experimental energy range.

The $\Delta\epsilon_1$ and $\Delta\epsilon_2$ spectra for W and Mo are shown in Figs. 2 and 3. The corresponding spectra for paramagnetic Cr (Ref. 7) are given in Fig. 4. Several features of the $\Delta\tilde{\epsilon}$ spectra show characteristic line shapes.[10,17] The typical derivative line shape[8,11,17] centered at 2.26 eV in Mo (Fig. 3), for example, is indicative of optical transitions involving the Fermi surface and the correlated $\Delta\epsilon_1$ and $\Delta\epsilon_2$ line shapes make the indentification unambiguous.

B. Tungsten

The dominant spectral feature in the $\Delta\tilde{\epsilon}$ spectra of W (Fig. 2) is a Fermi-surface transition at about 3.25 eV where the characteristic derivative $\Delta\epsilon_2$ line shape shows zero-crossing corresponding to a minimum of the typical $\Delta\epsilon_1$ line shape. An M_0 critical point is seen in $\Delta\epsilon_1$ and $\Delta\epsilon_2$ at about 2.45 eV while a smooth background[18] clearly underlies the

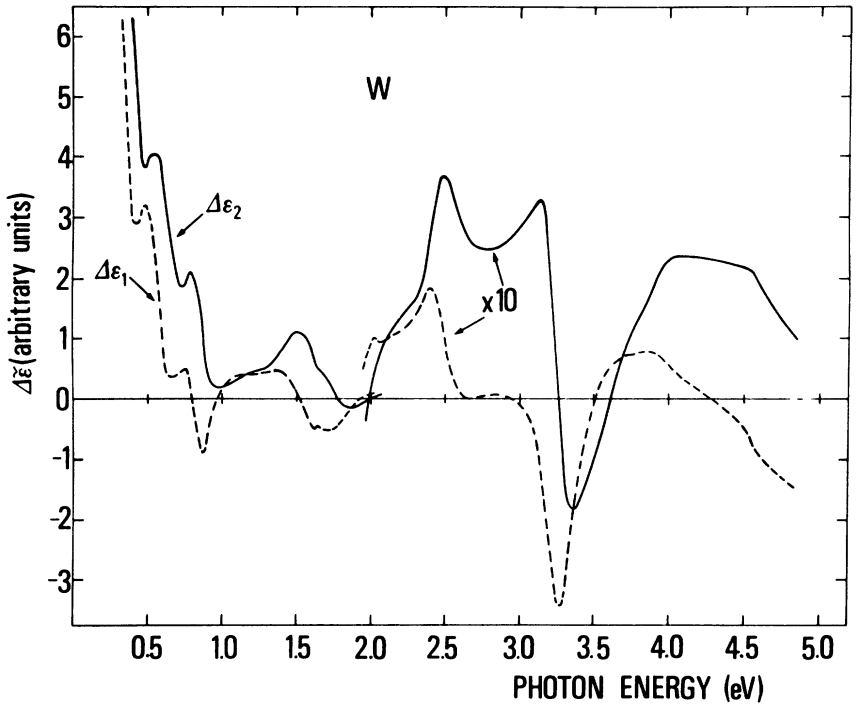

FIG. 2. Temperature-induced variation of the complex dielectric function $\tilde{\epsilon}$ for W. Solid line $\Delta\epsilon_2$. Dashed line $\Delta\epsilon_1$.

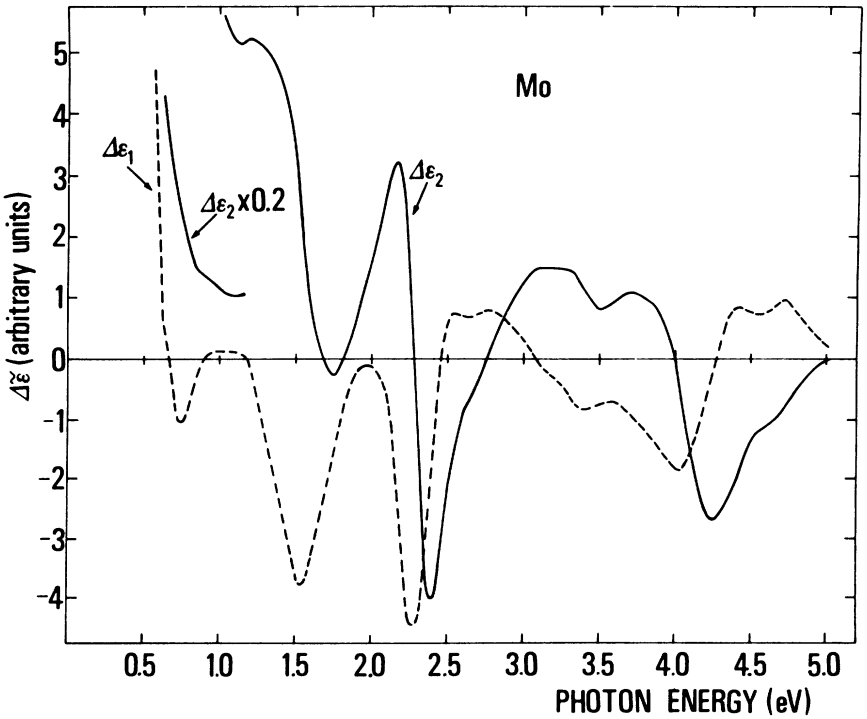

FIG. 3. Temperature-induced variation of the complex dielectric function $\tilde{\epsilon}$ for Mo. Solid line $\Delta\epsilon_2$. Dashed line $\Delta\epsilon_1$.

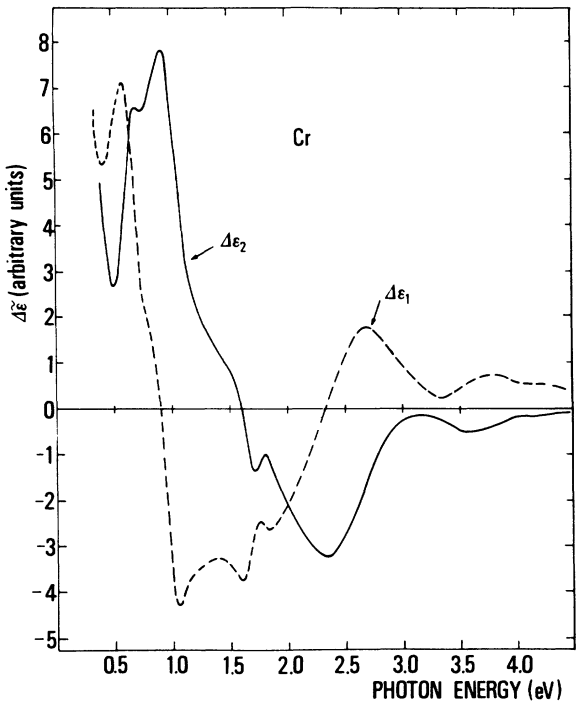

FIG. 4. Temperature-induced variation of the complex dielectric function $\tilde{\epsilon}$ for Cr. Solid line $\Delta\epsilon_2$. Dashed line $\Delta\epsilon_1$. (From Ref. 7.)

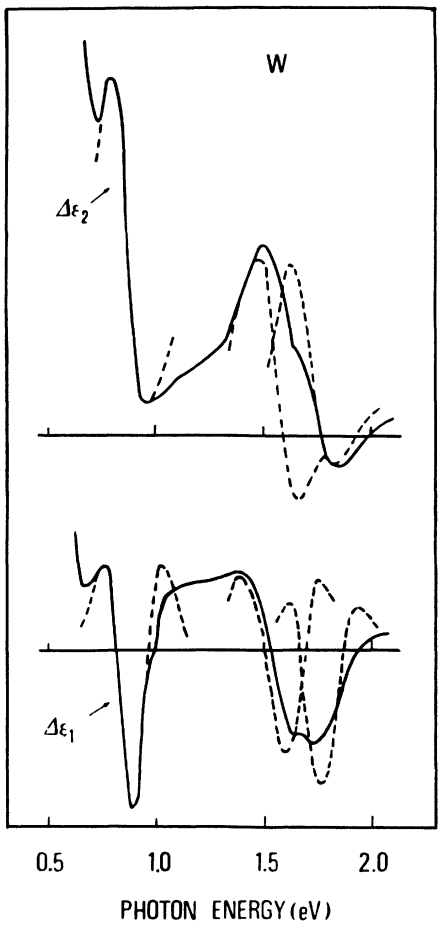

FIG. 5. Qualitative decomposition of $\Delta\epsilon_2$ (top) and $\Delta\epsilon_1$ (bottom) for tungsten in the low-energy range. Three Fermi-surface transitions at about 0.85, 1.60, and 1.75 eV contribute (dashed line) to the complex $\Delta\tilde{\epsilon}$ line shape.

whole high-energy region of the $\Delta\epsilon_2$ spectrum ($h\nu > 2$ eV).

In the low-energy range ($0.5 < h\nu < 2$ eV) a comparison of the $\Delta R/R$ and $\Delta\tilde{\epsilon}$ line shapes suggest several Fermi-surface transitions closely spaced in energy. A corresponding qualitative decomposition of $\Delta\tilde{\epsilon}$ (Fig. 5) shows Fermi-surface transitions at about 0.85, 1.6, and 1.75 eV. Other structures of more difficult interpretation appear both in $\Delta\tilde{\epsilon}$ and $\Delta R/R$ at 0.4 and 2.2 eV. The latter will be interpreted as an M_3 critical point through analysis of the Mo-W systematics.

C. Molybdenum

The main feature in the Mo spectra[19] corresponds to the Fermi-surface transition with onset at 2.26 eV. The broad structure at about 1.5 eV in $\Delta\tilde{\epsilon}$ is of composite nature as was previously suggested.[9] A qualitative decomposition of $\Delta\tilde{\epsilon}$ [Fig. 6(a)] shows two Fermi-surface transitions at 1.35 and 1.6 eV. The corresponding $\Delta R/R$ spectrum exhibits only one broad unresolved peak.

In the high-energy range an M_3 critical point at 4.6 eV is easily recognizable in $\Delta\epsilon_1$ and $\Delta\epsilon_2$. The $\Delta R/R$ and $\Delta\tilde{\epsilon}$ structures in the $3.5 < h\nu < 5.0$ eV photon-energy range show similarities with the spectral features in the $1.8 < h\nu < 2.9$ eV range (Figs. 1 and 3) and a qualitative decomposition of $\Delta\tilde{\epsilon}$ [Fig. 6(b)] indicates two Fermi-surface transitions at about 3.8 and 4.0 eV in addition to the M_3-type critical point at 4.6 eV. An analogous decomposition in the $1.8 < h\nu < 2.9$ eV range suggests a second M_3-type critical point at 2.7 eV (Fig. 3).

The $\Delta R/R$ spectra for Mo and W are qualitatively very similar in the energy ranges $2.5 < h\nu < 4.4$ eV and $1.9 < h\nu < 3.4$ (dashed intervals in Fig. 1). The Seraphin coefficients[10] are of equal sign and of the same order of magnitude so that a comparison of $\Delta R/R$ in the two cases is meaningful. The analogy suggests an M_0 critical point at 3.3 eV in Mo and an M_3 critical point at 2.2 eV in W that are not easily recognizable in the $\Delta\tilde{\epsilon}$ spectra.

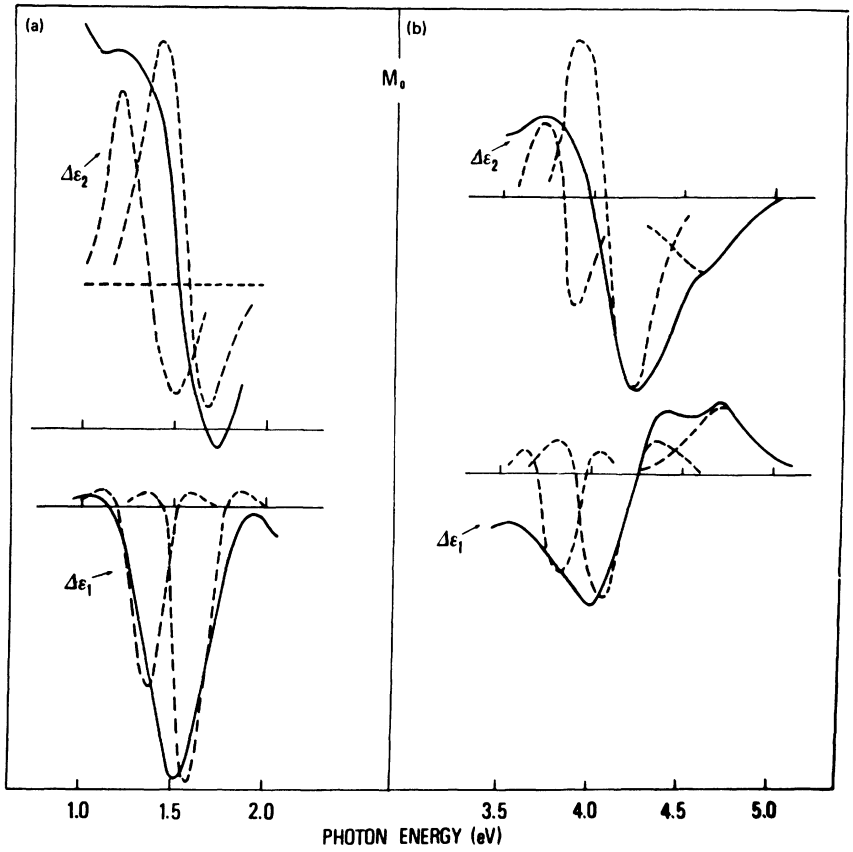

FIG. 6. (a) Qualitative decomposition of $\Delta\epsilon_2$ (top) and $\Delta\epsilon_1$ (bottom) for molybdenum in the low-energy range ($h\nu < 2.0$ eV). Two Fermi-surface transitions at about 1.35 and 1.60 eV contribute (dashed line) to the $\Delta\tilde{\epsilon}$ line shape. (b) Qualitative decomposition of $\Delta\epsilon_2$ (top) and $\Delta\epsilon_1$ (bottom) for molybdenum in the $3.5 < h\nu < 5.0$ eV photon-energy range. Two Fermi-surface transitions at 3.8 and 4.0 eV and an M_3 critical point at 4.6 eV account for the complex $\Delta\tilde{\epsilon}$ line shapes.

D. Chromium

The $\Delta R/R$ and $\Delta\tilde{\epsilon}$ spectra for paramagnetic Cr have been discussed elsewhere.[7] The spectral features below $h\nu = 2.0$ eV were interpreted all as Fermi-surface transitions. A number of critical points were identified (M_2, M_0, M_2, and M_3 type for increasing $h\nu$), in the $2 < h\nu < 4.2$ eV range. These identifications are summarized in Table I, together with the new results for Mo and W.[20]

In Fig. 7 we show the imaginary part ϵ_2 of the static dielectric constant $\tilde{\epsilon}$ as measured by Weaver *et al.* for Mo (Ref. 2) and W (Ref. 16) and by Bos and Lynch[21] for Cr. The main contributions to the optical absorption identified through thermoreflectivity in this work (Table I) are shown for comparison (vertical arrows). Figure 7 clearly demonstrates how modulation techniques yield a more detailed analysis of the optical properties of solids. Transitions involving the Fermi surface are emphasized in thermoreflectance experiments through the modulation of the Fermi distribution and can be seen through standard optical techniques only if the joint density of states (JDOS) is sufficiently high. Furthermore, the corresponding thermoreflectance spectra exhibit a characteristic sharp derivative line shape at the onset of the transitions (Figs. 1–6) where ϵ_2 generally shows only a broad structure centered around the JDOS discontinuity.

IV. DISCUSSION

A. Calculations

We will compare our experimental data to the calculations by Christensen and Feuerbacher[22] for tungsten (Fig. 8) and by Koelling *et al.*[23] for molybdenum (Fig. 9). Although the choice of the potential was driven by different criteria, the authors used the same relativistic augmented-plane-wave (RAPW) method. This will emphasize the sys-

TABLE I. Interband transitions in W, Mo, and Cr as identified through thermoreflectance in this work. Both the experimental energy of the onset and the proposed localization of the transitions in the Brillouin zone are given in the table.

Energy (eV)	Identification (Ref. 26)
Tungsten	
0.85	Fermi surface $G^{(3)}\rightarrow G^{(4)}$
1.60	Fermi surface $\Delta_7(E_F)\rightarrow\Delta_7$
1.75	Fermi surface $\Delta_6(E_F)\rightarrow\Delta_7$
2.20	M_3 critical point $\Gamma_7^+\rightarrow\Gamma_8^+$
2.45	M_0 critical point $G^{(2)}\rightarrow G^{(4)}$
3.25	Fermi surface $\Delta_7(E_F)\rightarrow\Delta_6$; $\Delta_6(E_F)\rightarrow\Delta_6$
Molybdenum	
1.35	Fermi surface $\Sigma^{(3)}\rightarrow\Sigma^{(4)}(E_F)$
1.60	Fermi surface $\Sigma^{(3)}(E_F)\rightarrow\Sigma^{(4)}$
2.26	Fermi surface $\Sigma^{(3)}(E_F)\rightarrow\Sigma^{(5)}$
2.70	M_3 critical point $\Gamma_7^+\rightarrow\Gamma_8^+$
3.30	M_0 critical point $G^{(2)}\rightarrow G^{(4)}$
3.80	Fermi surface $\Delta_7(E_F)\rightarrow\Delta_6$
4.00	Fermi surface $\Delta_6(E_F)\rightarrow\Delta_6$
4.60	M_3 critical point $N^{(2)}\rightarrow N^{(3)}$
Chromium	
0.80	Fermi surface $G_3(E_F)\rightarrow G_1$; $G_4(E_F)\rightarrow G_1$
1.00	Fermi surface $\Sigma_1\rightarrow\Sigma_3(E_F)$; $\Lambda_1(E_F)\rightarrow\Lambda_3$
1.40	Fermi surface $\Sigma_1(E_F)\rightarrow\Sigma_1$; $D_3(E_F)\rightarrow D_1$; $\Sigma_1\rightarrow\Sigma_1(E_F)$; $\Delta_5(E_F)\rightarrow\Delta_2'$
1.60	Fermi surface $\Sigma_1(E_F)\rightarrow\Sigma_4$; $D_3(E_F)\rightarrow D_2$
2.30	M_2 critical point $\Sigma_1\rightarrow\Sigma_3$
2.84	M_0 critical point along G
3.42	M_2 critical point along Σ, Λ, or F
3.66	M_3 critical point $N_2\rightarrow N_1'$

tematic trends. Koelling *et al.*[23] calculated the contribution to the JDOS from interband transitions which either originate or terminate within an energy window ΔE from the Fermi level. Their results may be compared to our measurements that enhance the interband transitions involving E_F. (The calculations, however, assume constant matrix element.)

To our knowledge no relativistic band-structure calculations exist for Cr. We will use recent results by Laurent *et al.*[24] (Fig. 10) that are in good agreement with photoemission and de Haas–van Alphen data.

B. Critical-point transitions

In a previous paper[7] we showed that the M_2-type critical point at 2.30 eV in Cr occurs along high-symmetry lines of the bcc Brillouin zone. Through the systematics we attribute now this critical point to transitions $\Sigma_1\rightarrow\Sigma_2$ between parallel bands about the midpoint of the Γ-N direction where Σ_1 is still a mixture of s-, p-, and d-like levels.[25] In fact, Christensen and Feuerbacher[22] explicitly forecast an M_2 critical point along Σ in tungsten. This critical point should occur at 3.30 eV in W and, by analogy, at about 2.2 eV in Mo. In both metals we observe strong derivative $\Delta\epsilon_2$ line shapes indicating transitions involving the Fermi surface (2.26 eV in Mo and 3.25 eV in W). These may hide a weaker M_2-type contributions.

We identify the M_0 critical point at 2.45 eV in W as due to transitions between bands 2 and 4 along G.[26] The k dependence and the energy separation support this identification. Its counterpart in molybdenum occurs at 3.3 eV in rough agreement with band-structure calculations (2.8 eV in Fig. 9 for $G^{(2)}\rightarrow G^{(4)}$ transitions).[26] For Cr, band 2 and 3 along G will be separated by a small energy gap if relativistic effects are taken into account so that transitions $G^{(2)}\rightarrow G^{(4)}$ could then explain the M_0 critical point observed experimentally at 2.84 eV.

Static optical data for Mo (Ref. 2) and Cr (Ref. 21) fail to reveal absorption features in these energy ranges, while for W (Ref. 16) a maximum in ϵ_2 was

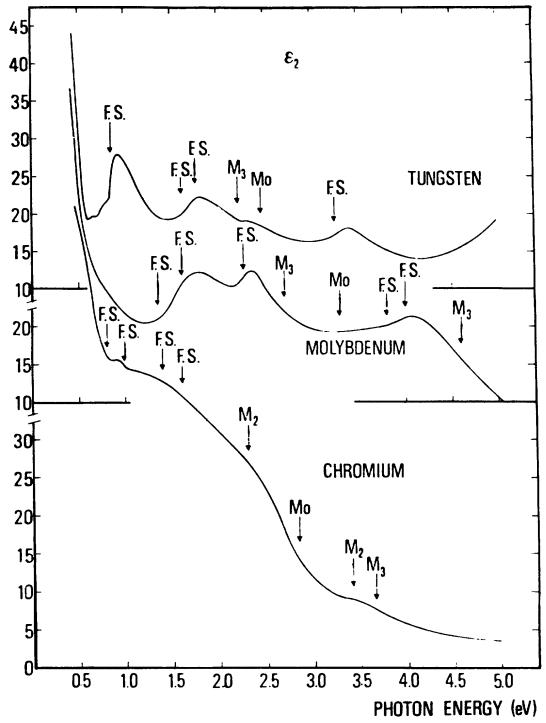

FIG. 7. Imaginary part ϵ_2 of the complex dielectric constant $\tilde{\epsilon}$ for tungsten (From Ref. 16), molybdenum (from Ref. 2), and chromium (from Ref. 21). The arrows mark the positions of the interband absorption features identified through thermoreflectance in this work. The type of absorption line shape—M_0, M_1, M_2, or M_3 critical points or transitions involving the Fermi surface (FS)—from Table I is also indicated in the figure.

observed at 2.35 eV. Weaver *et al.*[16] interpreted this feature as deriving from Fermi-surface transitions along $\Gamma(\Delta)H$ but the analysis of the thermoreflectance line shape tends to rule out this attribution.

The existence of an M_3 critical point at $N(N_2 \rightarrow N_1')$ seems a general aspect of transition metals. We showed[1] that such a critical point is easily observed in the group-V*B* elements through thermomodulation experiments since the deformation potential of the N_1' level is large.[27] We observe an M_3 critical point at 3.66 eV in Cr and at 4.6 eV in molybdenum, in remarkable good agreement with theory (3.5 and 4.6 eV, respectively, in Figs. 10 and 9 for the $N_2 \rightarrow N_1'$ transition energy). Such a critical point is not apparent in our tungsten data but we note first that very few empty states are present in band 3 at N for W so that we expect a reduced JDOS for the $N_2 \rightarrow N_1'$ transition. Second, the theory predicts the onset of the transitions at about 3.2 eV where a sharp Fermi-surface transition line dominates our spectra.

The only possible candidates for the M_3 critical point at 2.2 eV in Mo and 2.7 eV in W seem to be transitions near Γ between band 4 and 5, although transitions $\Gamma_7^+ \rightarrow \Gamma_8^+$ are dipole forbidden. Both the $\vec{k}$ dependence of the bands near Γ and the theoretical energy separation (2.6 eV for Mo and 2.4 eV for W in Figs. 9 and 8, respectively) support this interpretation. The corresponding critical point in Cr should occur at about 2 eV where other important absorption features dominate the $\Delta\tilde{\epsilon}$ spectra. The absorption at Γ should disappear in the V-group metals when the Γ_{25}' states are above the Fermi level and, indeed, no such critical point was observed in the V-Nb-Ta series.[1]

C. Fermi-surface transitions

Fermi-surface transitions appear at 3.25 eV in W and at 3.8 and 4.0 eV in Mo. They are all associated with $\Delta_7(E_F) \rightarrow \Delta_6$ and $\Delta_6(E_F) \rightarrow \Delta_6$ transitions that

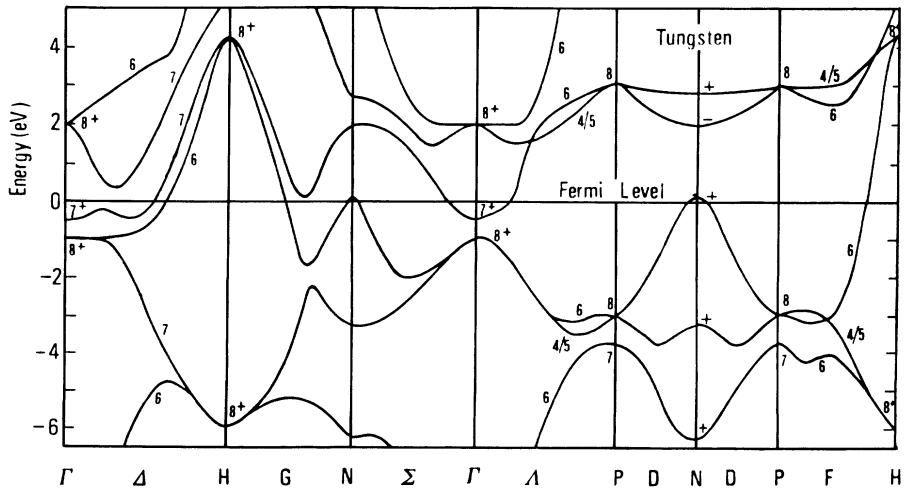

FIG. 8. Tungsten band structure from Christensen and Callaway (Ref. 22).

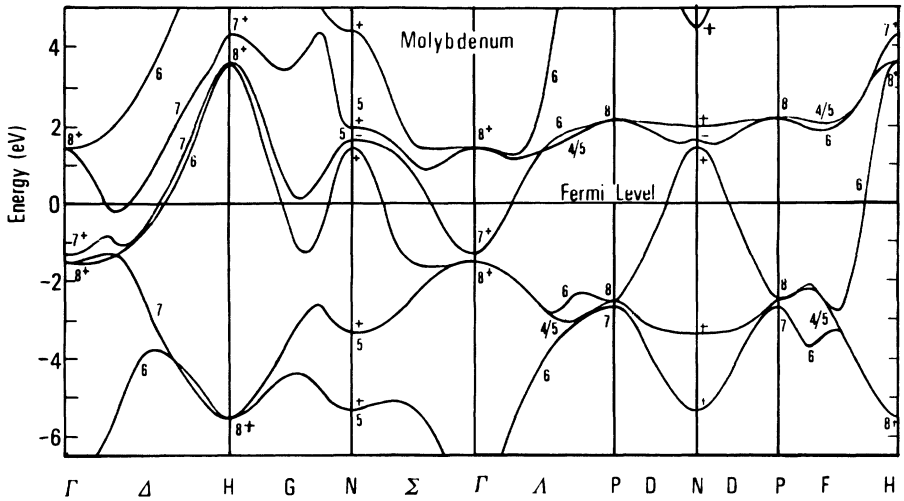

FIG. 9. Molybdenum band structure from Koelling *et al.* (Ref. 23).

are degenerate in energy in W where the final Δ_6 level is rather flat. In molybdenum such transitions occur between largely parallel bands so that we observe two derivative line shapes with energy separation of the order of the spin-orbit splitting. The corresponding transitions on Cr are expected at about 3 eV but are not apparent in our spectra,[7] where critical-point absorption features dominate.[28]

Fermi-surface absorption features at 1.6 and 1.75 eV in W have the $\Delta_7(E_F)\rightarrow\Delta_7$ and $\Delta_6(E_F)\rightarrow\Delta_7$ transitions as only candidates along symmetry lines.[29] Bands 3, 4, and 5 are parallel[22] along Δ so that the expected energy difference of the transitions is of the same order of magnitude of the relativistic splitting and slightly larger ($\sim$0.4 eV) of the experimental value (0.15 eV). Weaver *et al.*[16] previously associated the $\Delta_7(E_F)\rightarrow\Delta_7$ and $\Delta_6(E_F)\rightarrow\Delta_7$ transitions with ϵ_2 features at 1.82 and 2.35 eV, respectively. Our data, however, show no evidence of Fermi-surface transitions at 2.35 eV. We note, instead, that both the M_3 critical point at 2.2 and the M_0 critical point at 2.45 could be associated (Fig. 7) with the observed ϵ_2 feature.

By analogy with the W case, it would be tempting to associate the Fermi-surface transitions observed in Mo at 1.3 and 1.6 eV with the $\Delta_7(E_F)\rightarrow\Delta_7$ and $\Delta_6(E_F)\rightarrow\Delta_7$ transitions.[30] However, we have to discount this interpretation since it is inconsistent with the systematics of thermoreflectance in the $Nb_{1-x}Mo_x$ alloy series.[9] Several new transitions, in fact, occur in Mo as opposed to W in this energy range and other candidates are transitions along G (near N) and along Σ_1. In alloying with Nb (i.e., lowering the Fermi level) transitions[26] $\Sigma^{(3)}(E_F)\rightarrow\Sigma^{(4)}$ are expected to shift to higher energy while the opposite trend is expected for the $\Sigma^{(3)}\rightarrow\Sigma^{(4)}(E_F)$ transitions. Experimentally, Fermi-surface absorption features at 1.35 and 1.6 eV follow this double trend[9] so that transitions along Σ are the most likely candidates.[30]

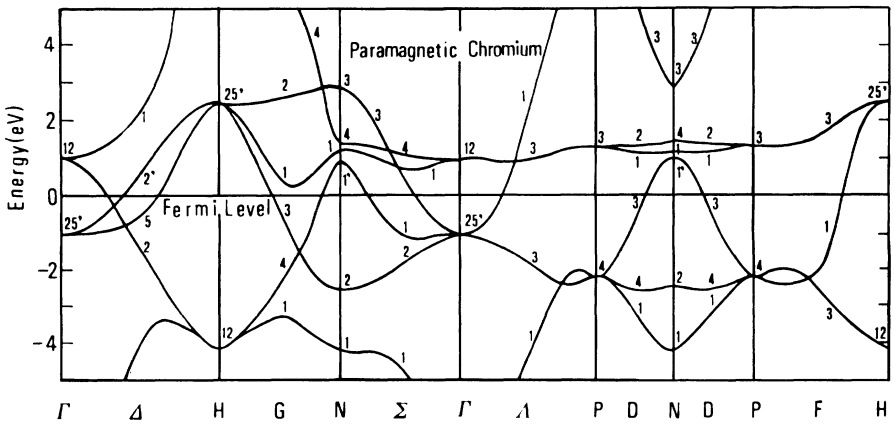

FIG. 10. Paramagnetic chromium band structure from Laurent *et al.* (Ref. 24).

We observe Fermi-surface transitions for Cr in the same energy range at 1.0, 1.4, and 1.6 eV.[7] A look at the band structure of Fig. 10 shows a number of possible candidates close in energy to one another. Several attributions can be done on the basis of the changes induced by the paramagnetic to antiferromagnetic phase transition.[7] The transition $\Sigma_1 \rightarrow \Sigma_3(E_F)$, for example, contributes to the structure at 1.0 eV in Cr and shifts to 1.35 eV in Mo while it has negligible intensity in W where the joint density of states is lower. Our identifications are summarized in Table I.

In the high photon-energy range ($h\nu \geq 2.0$ eV) the systematic in the Cr-Mo-W series confirms the conclusion[9,32] that transitions along Σ are mainly responsible for the Fermi-level absorption features. The derivative line shape at 2.26 eV in Mo (Fig. 1) does not shift in energy in alloying with Nb[9] indicating transitions between parallel bands. This rules out the $\Delta_7(E_F) \rightarrow \Delta_6$ transitions that tend to disappear in alloying with Nb and supports instead, transitions along Σ. The $\Sigma^{(3)}(E_F) \rightarrow \Sigma^{(5)}$ transitions,[26] in particular, are at about 1.9–2.0 eV in Mo (Fig. 9), shift at 1.6 eV in Cr, and disappear in W where the initial states fall to much higher binding energy, in agreement with the experimental systematics.

In the low-energy spectral range ($h\nu \leq 1.0$ eV), Fermi-surface transitions are observed for Cr and W (0.8 and 0.85 eV, respectively) but not for Mo. The calculations suggest two possible candidates: Transitions $\Delta_6(E_F) \rightarrow \Delta_7$ should occur at slightly lower energy (0.5 eV) in W, disappear in Mo (where the relativistic splitting is lower and the structure shifts out of the experimental range), and change to transitions $\Delta_5(E_F) \rightarrow \Delta_2'$ in Cr (~ 1.2 eV in Fig. 10). Alternatively, transitions $G_3(E_F) \rightarrow G_1$ should occur at about 0.8 eV in Cr,[33] at about 1.0 eV in W, and at lower energy (possibly out of the experimental range) in Mo, so that both identifications are consistent with the experimental trend. We favor the $G_3(E_F) \rightarrow G_1$ transitions because the observed onset for the transition in W (0.85 eV) is higher than the expected relativistic splitting of band Δ_5.[34]

V. CONCLUSIONS

The analysis of the systematic trends of the thermoreflectance spectra of Cr-group metals allowed us to unambiguously explain most optical features in the $0.5 < h\nu < 5.0$ eV photon-energy range. Our results confirm and extend substantially the general picture introduced in previous thermoreflectance works such as our study of the optical properties of Cr below and above the Néel temperature, the study of the Nb-Mo alloy system, and of the V-group metals. We believe that the present work is an important step forward in the general understanding of the electronic properties of transition metals. Additional band-structure calculations suitable for estimating the dipole matrix elements and for searching critical points in the BZ are needed to clarify a few controversial issues.

[1] R. Rosei, E. Colavita, A. Franciosi, J. H. Weaver, and D. T. Peterson, Phys. Rev. B 21, 3152 (1980).

[2] J. H. Weaver, D. W. Lynch, and C. G. Olson, Phys. Rev. B 10, 501 (1974).

[3] J. H. Weaver, in *Physics of Transition Metals,* edited by M. J. G. Lee, J. H. Perz, and E. Fawcett (Institute of Physics and Physical Society, London, 1978), pp. 115–127.

[4] A large number of references on the optical properties of transition metals can be found in J. H. Weaver, C. Krafka, D. W. Lynch, and E. E. Koch, *Optical Properties of Metals,* Physik Daten/Physics Data No. 18-1 and 18-2 (Fach-Informations-Zentrum, Energie Physick Mathematik GmbH, Karlsruhe, 1981).

[5] References to experimental and theoretical results for Mo and W can be found in the following: J. H. Weaver, D. W. Lynch, and C. G. Olson, Phys. Rev. B 10, 501 (1974) (Mo); B. W. Veal and A. P. Paulikas, *ibid.* 10, 1280 (1974) (Mo); D. D. Koelling, F. M. Mueller, and B. W. Veal, *ibid.* 10, 1290 (1974) (Mo); N. E. Christensen and B. Feuerbacher, *ibid.* 10, 2349 (1974) (W); J. H. Weaver, C. G. Olson, and D. W. Lynch, *ibid.* 12, 1293 (1975) (W); J. Yamashita, Y. Kubo, and S. Wakoh, J. Phys. Soc. Jpn. 42, 1906 (1977) (Mo); J. E. Nestell Jr. and R. W. Christy, Phys. Rev. B 21, 3173 (1980) (Mo and W).

[6] A large number of references on the optical properties of Cr can be found in E. Colavita, A. Franciosi, D. W. Lynch, G. Paolucci, and R. Rosei (unpublished) and H. L. Skriver, J. Phys. F. 11, 97 (1981).

[7] E. Colavita, A. Franciosi, D. W. Lynch, G. Paolucci, and R. Rosei (unpublished).

[8] E. Colavita, S. Modesti, and R. Rosei, Phys. Rev. B 14, 4315 (1976); E. Colavita, G. Paolucci, and R. Rosei (unpublished).

[9] E. Colavita, E. Franciosi, R. Rosei, F. Sacchetti, E. S. Giuliano, R. Ruggeri, and D. W. Lynch, Phys. Rev. B 20, 4864 (1979).

[10] M. Cardona, *Modulation Spectroscopy,* Suppl. 11 to *Solid State Physics,* edited by F. Seitz, D. Turnbull, and H. Ehrenreich (Academic, New York, 1969); B. Batz, *Semiconductors and Semimetals,* edited by R. K. Willardson and A. C. Beer (Academic, New York, 1972), Vol. 9, p. 316.

[11] J. H. Weaver, D. W. Lynch, C. H. Culp, and R. Rosei, Phys. Rev. B 14, 459 (1976).

[12]L. F. Mattheiss, Phys. Rev. 134, A970 (1964); L. Hodges, R. E. Watson, and H. Ehrenreich, Phys. Rev. B 5, 3953 (1972); A. R. Mackintosh and O. K. Andersen, in *Electrons at the Fermi Surface,* edited by M. Springford (Cambridge University Press, London, 1980), Chap. 5, p. 149.

[13]J. H. Weaver, C. G. Olson, D. W. Lynch, and M. Piacentini, Solid State Commun. 16, 163 (1975).

[14]H. Dallaporta, J. H. Debever, and J. Hanus, Nuovo Cimento 39B, 455 (1977).

[15]E. Colavita, G. Falasca, G. Paolucci, and R. Rosei (unpublished) and Ref. 9.

[16]J. H. Weaver, C. G. Olson, and D. W. Lynch, Phys. Rev. B 12, 1293 (1975).

[17]R. Rosei, Phys. Rev. B 10, 474 (1974); M. Guerrisi, R. Rosei, and P. Winseimius, *ibid.* 12, 557 (1975).

[18]Such a background does not vary if the experimental $\Delta R/R$ baseline is shifted [A. Balzarotti, E. Colavita, S. Gentile, and R. Rosei, Appl. Opt. 14, 2412 (1975)] and may come from several unresolved contributions to the optical absorption.

[19]A preliminary analysis of the Mo data was used in Ref. 9 to interpret thermomodulation data for Nb_xMo_{1-x} alloys.

[20]We emphasize that the M_0-type critical points at 2.84 eV in Cr, 3.30 eV in Mo, and 2.45 eV in W give contributions of opposite sign to $\Delta R/R$ (positive in Mo and W, negative in Cr), because of the different sign and magnitude of the Seraphin coefficients. This is an example of how dangerous it is to interpret directly $\Delta R/R$ in terms of critical-point transitions.

[21]L. W. Bos and D. W. Lynch, Phys. Rev. B 2, 4567 (1970).

[22]N. E. Christensen and B. Feuerbacher, Phys. Rev. B 10, 2349 (1974).

[23]D. D. Koelling, F. M. Mueller, and B. W. Veal, Phys. Rev. B 10, 1290 (1974).

[24]D. G. Laurent, J. Callaway, J. L. Fry, and N. E. Brener, Phys. Rev. B 23, 4977 (1981).

[25]This transition could correspond to the absorption feature that Nestell and Christy (Ref. 5) observe at 2.0 eV and that they interpret as due to interband transitions between 3 and 4 in general.

[26]No ambiguous relativistic notation is shown in the literature (Refs. 22 and 23) for the representations along the symmetry lines G, Σ, and D. We choose here the usual convention of numbering the bands in Figs. 8 and 9 from bottom to top so that the transitions between the second and the fourth band along G, for example, are simply indicated as $G^{(2)} \rightarrow G^{(4)}$.

[27]We found in Ref. 9 that a variation of the Nb lattice parameter of 3% yields a 0.85 eV change of the $N_2 \rightarrow N_1'$ gap.

[28]This suggests a reduction of the oscillator strength for these transitions. In fact (Fig. 10), the corresponding bands may not run parallel for a relevant portion of k space, as compared with Mo and W.

[29]Based on matrix elements and joint density-of-states arguments.

[30]Koelling *et al.* (Ref. 23) calculated a rather high joint density of states for such transitions in molybdenum.

[31]This agrees with our previous conclusion of Ref. 9. There we discussed the Nb_xMo_{1-x} data in terms of nonrelativistic band structures and identified the $\Sigma_1(E_F) \rightarrow \Sigma_1$ and $\Sigma_1 \rightarrow \Sigma_1(E_F)$ transitions as the most likely candidates.

[32]The attribution was correctly made in the text (Ref. 9, p. 4864) but appears incorrect in the abstract due to misprinting (transitions along G are indicated in the abstract).

[33]Transitions $G_4(E_F) \rightarrow G_1$ occur at almost the same energy in Cr. Although they have no counterpart in Mo and W (this can be argued through systematics), they have to be taken into account to explain the changes in the optical spectra driven by the antiferromagnetic to paramagnetic phase transition.[7]

[34]Thermomodulation measurements at lower photon energy could discriminate between the two identifications by ascertaining the nature of the $\Delta R/R$ structure at 0.8 eV in Mo and 0.4 in W.